Journal of The Magnetics Society of Japan Vol.21, Supplement, No.S2 (1997)

PRML Systems for Perpendicular Magnetic Recording

Hisashi OSAWA[1], Yoshitake KURIHARA[2], Yoshihiro OKAMOTO[1], Hidetoshi SAITO[1], Hiroaki MURAOKA[3] and Yoshihisa NAKAMURA[3]

1)Ehime Univ., 3 Bunkyo-cho, Matsuyama, Ehime 790 Japan
2)Niihama Nat. Col. Tech., 7-1 Yagumo-cho, Niihama, Ehime 792 Japan
3)Tohoku Univ., 2-1-1 Katahira, Aoba-ku, Sendai, Miyagi 980 Japan

Abstract— Partial response maximum-likelihood(PRML) systems using an MR head and a double layer perpendicular medium are studied. The bit-error rate performance of PRML systems characterized by the polynomials with the positive coefficients for the (1,7) code and the negative coefficients for the 8/9 code is evaluated. The PRML system for the (1,7) code has a large minimum Euclidean distance and a small noise spectrum compared with those for the 8/9 code. This results in a significant performance improvement. Among PRML systems discussed in this study, PR(1, 2, 3, 2, 1)ML exhibits the best performance and improves the SNR by about 13.8 dB over that of PR4ML for the 8/9 code at a bit-error rate of 10^{-4} and a normalized linear density of 2.5. PR(1, 2, 2, 1)ML, PR(1, 3, 3, 1)ML and PR(1, 2, 1)ML also show excellent performance.

Key words: PRML system, MR head, double layer perpendicular medium, BER performance

I. INTRODUCTION

Signal processing technologies have played a significant role in the remarkable increases in data storage density of longitudinal magnetic recording systems. Especially, the partial response maximum-likelihood (PR ML) system, i.e., partial response signaling combined with maximum-likelihood sequence detection, is considered to be an indispensable signal processing method for high-density recording [1]–[3].

Recently the combination of an MR head and a perpendicular disk has received much attention as a promising technology for future high-density recording [4]–[8]. With the PRML system for such a combination, only systems using a single layer medium [9] and a multilayer medium [8] have been studied.

In this study, our discussion will be focused on PRML systems using an MR head and a double layer perpendicular medium. The isolated reproducing waveform from a double layer medium is characterized by a step function [5], [6], [10]. Then, the reproducing waveform for the rectangular recording waveform becomes a rectangular pulse-like waveform. In the case of the longitudinal magnetic recording with differential characteristics, the PRML systems expressed by the polynomials with the negative coefficients, e.g., PR(1,0,−1)ML (PR4ML), PR(1,1, −1, −1)ML (EPR4ML), PR(1, 2, 0, −2, −1)ML (E^2PR4ML) and PR(1, 1, 0, −1, −1)ML (ME^2PR4ML) [11], provide good performance, while in our case without differential characteristics, PR(1, 2, 1)ML, PR(1, 2, 2, 1)ML, PR(1, 3, 3, 1)ML and PR(1, 2, 3, 2, 1)ML characterized by the polynomials with the positive coefficients are expected to show excellent performance.

Here, the rate 2/3 (1,7) code or the rate 8/9 (0, 4/4) code as a recording code is employed. The maximum-likelihood sequence detector is usually implemented as a Viterbi detector. For the PRML systems with the positive coefficients, the Viterbi detector utilizing the minimum run-length constraint of the (1,7) code has larger minimum Euclidean distance $d_{\min}$ between all possible pairs of sequences at the input of the detector than that for the 8/9 code. The increase in $d_{\min}$ brings a performance improvement. On the other hand, it is favorable for the PRML systems with the negative coefficients to use the 8/9 code having a large coding rate compared with the (1,7) code.

In this study, the bit-error rate (BER) performance of PRML systems with the positive coefficients for the (1,7) code and the negative coefficients for the 8/9 code is evaluated by computer simulation. The relationship between the SNR improvement over PR4ML and the linear density is also studied.

II. RECORDING/REPRODUCING SYSTEM

Fig.1 shows the PRML system in perpendicular magnetic recording. $\{a_{k'}\}$ is the input data sequence at time $k'T_b$, and $\{b_k\}$ is the (1,7) code or the 8/9 code sequence at time kT_s, where k' and k are integers, T_b is the bit interval and T_s is the symbol interval. For the

(1,7) code, the precoded sequence $\{c_k\}$ is equivalent to the NRZI recorded sequence and is related to $\{b_k\}$ by

$$c_k = b_k + c_{k-1} \qquad (\text{mod } 2)\ . \tag{1}$$

The precoder of each PRML system for the 8/9 code and the maximum run-length of 0's in the output sequence $\{d_k\}$ of the equalizer are shown in Table 1. Since the isolated reproducing waveform is step function-like [5], [6], [10], its differentiated waveform is assumed to be Lorentzian given by

$$h(t) = \frac{B}{1 + (2t/T_{50})^2} \tag{2}$$

where B is the peak value and T_{50} is the half height width. By integrating $h(t)$, the signal waveform at the reading point for the recording waveform with height 1 and pulse width T_s corresponding to a recording data "1" is obtained as follows:

$$\begin{aligned} g(t) &= \frac{A}{2\tan^{-1}(\eta_c/K_p)} \\ &\quad \cdot \left\{ \tan^{-1}\frac{2\eta_c t}{K_p T_s} - \tan^{-1}\frac{2\eta_c(t-T_s)}{K_p T_s} \right\} \end{aligned} \tag{3}$$

where A is the peak value of $g(t)$, $\eta_c = T_s/T_b$ is the coding rate and $K_p = T_{50}/T_b$ is the normalized linear density. η_c's for the (1,7) and 8/9 codes are 2/3 and 8/9, respectively.

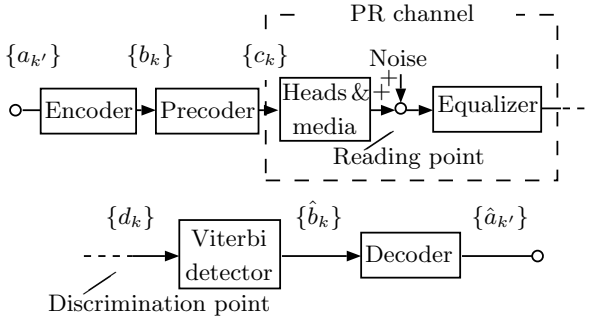

Fig. 1 Block diagram of PRML system.

Table 1 Precoders of PRML systems for the 8/9 code and the maximum run-lengths of 0's in $\{d_k\}$.

PRML system	Precoder (mod 2)	Maximum run-length
PR4ML	$c_k = b_k + c_{k-2}$	4
EPR4ML	$c_k = b_k + c_{k-2}$	3
E^{2}PR4ML	$c_k = b_k + c_{k-2}$	2
ME^{2}PR4ML	$c_k = b_k + c_{k-1} + c_{k-3} + c_{k-4}$	4

Assume that the noise at the reading point is a zero-mean, white Gaussian noise with two-sided power spectral density $N_0/2$. The transfer function of the equalizer is determined so that the output waveform $w(t)$ of the equalizer for $g(t)$ has the desired partial response characteristics PR(u_0, u_1, u_2, $\cdots$, u_{L-1}):

$$w(t) = \frac{1}{2}\sum_{m=0}^{L-1} u_m r(t - mT_s) \tag{4}$$

where $r(t)$ is the Nyquist waveform with a roll-off factor β given by

$$r(t) = \frac{\sin(\pi t/\eta T_b)}{\pi t/\eta T_b} \cdot \frac{\cos(\pi\beta t/\eta T_b)}{1 - (2\beta t/\eta T_b)^2}\ . \tag{5}$$

Here, η is a parameter which prescribes the amount of intersymbol interference and the bandwidth of the equalizer [12]. With increasing η, the intersymbol interference increases, but the bandwidth, and hence the noise power at the discrimination point, decreases.

Taking the ratio of the Fourier transform of $w(t)$ to the Fourier transform of $g(t)$, we have the transfer function of the equalizer:

$$\begin{aligned} E(x) &= \frac{\tan^{-1}(\eta_c/K_p)}{A} \cdot \frac{xR(x)e^{\pi K_p|x|}}{\sin(\pi\eta_c x)} \\ &\quad \cdot \sum_{m=0}^{L-1} u_m \mathrm{e}^{-j(2m-1)\pi\eta_c x} \end{aligned} \tag{6}$$

where x is the frequency normalized by the bit rate f_b. $R(x)$ is the Fourier transform of $f_b r(t)$ and is given by

$$R(x) = \begin{cases} \eta & ,|x| < \frac{1-\beta}{2\eta} \\ \frac{\eta}{2}\left\{1 - \sin\frac{\eta\pi}{\beta}\left(|x| - \frac{1}{2\eta}\right)\right\} & \\ & ,\frac{1-\beta}{2\eta} \le |x| < \frac{1+\beta}{2\eta} \\ 0 & ,|x| \ge \frac{1+\beta}{2\eta} \end{cases} . \tag{7}$$

For the PRML systems with the negative coefficients, such as PR4ML, EPR4ML, E^{2}PR4ML and ME^{2}PR4ML, it can be shown that $E(x)$ is equal to the transfer functions of these PRML systems in longitudinal magnetic recording multiplied by the transfer function x of the differentiator. Therefore, the PRML systems with the negative coefficients in perpendicular magnetic recording are equivalent to the differential equalizer combined with those in longitudinal magnetic recording.

Table 2 Postcoders of PRML systems for the 8/9 code.

PRML system	Postcoder (mod 2)
PR4ML	$\hat{b}_k = \hat{c}_k + \hat{c}_{k-2}$
EPR4ML	$\hat{b}_k = \hat{c}_k + \hat{c}_{k-2}$
E^{2}PR4ML	$\hat{b}_k = \hat{c}_k + \hat{c}_{k-2}$
ME^{2}PR4ML	$\hat{b}_k = \hat{c}_k + \hat{c}_{k-1} + \hat{c}_{k-3} + \hat{c}_{k-4}$

For the (1,7) code, the output sequence $\{\hat{b}_k\}$ of the postcoder with the inverse precoding operation is given by

$$\hat{b}_k = \hat{c}_k + \hat{c}_{k-1} \qquad \text{(mod 2)} \tag{8}$$

where $\{\hat{c}_k\}$ is the estimate of $\{c_k\}$. The postcoders of PRML systems for the 8/9 code are shown in Table 2. These postcoding operations can be taken into account in Viterbi detector. $\{\hat{b}_k\}$ is decoded by the (1,7) or 8/9 decoder, which gives the output data sequence $\{\hat{a}_{k'}\}$.

III. EYE PATTERNS

The signal waveform at the discrimination point for the precoder output $\{c_k\}$ is given by

$$y(t) \quad = \quad \sum_i (2c_i - 1)w(t - iT_s) \ . \tag{9}$$

Eye patterns obtained by computer simulation are shown in Figs. 2 and 3. In simulation, the input data sequence generated from M-sequence is coded into the (1,7) code or 8/9 code and the precoded sequence $\{c_k\}$ is used in Eq.(9). Fig.2 shows the eye patterns of PR(1, 2, 1)ML, PR(1, 2, 2, 1)ML, PR(1, 3, 3, 1) and PR(1, 2, 3, 2, 1)ML for the (1,7) code. Fig.3 shows the eye patterns of PR4ML, EPR4ML, E^{2}PR4ML and ME^{2}PR4ML for the 8/9 code. Here, $\beta = 0.5$ and $\eta = \eta_{\rm opt}$. $\eta_{\rm opt}$ is the optimum value of η which gives the minimum BER. When $\eta = \eta_{\rm c}$, the positive, outside signal level at $t = kT_s$ in the eye pattern takes only one value e_0. However, when $\eta > \eta_{\rm c}$, the level has a distribution due to the intersymbol interference. Since the middle value e_1 of the distribution increases with η, all eye patterns in Fig.2 are normalized by multiplying e_0/e_1 for the convenience of performance comparison. As can be seen in Figs. 2 and 3, PR(1, 2, 2, 1)ML, PR(1, 3, 3, 1)ML and

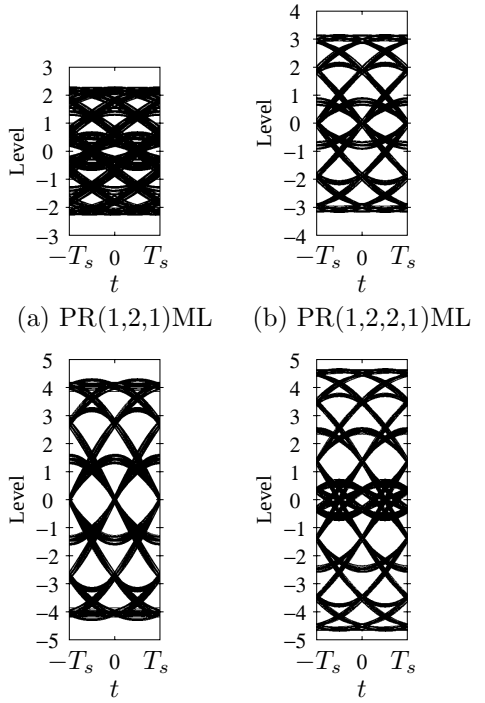

(a) PR(1,2,1)ML (b) PR(1,2,2,1)ML

(c) PR(1,3,3,1)ML (d) PR(1,2,3,2,1)ML

Fig. 2 Eye patterns of PRML systems for the (1,7) code ($\beta = 0.5$, $\eta = \eta_{\rm opt}$).

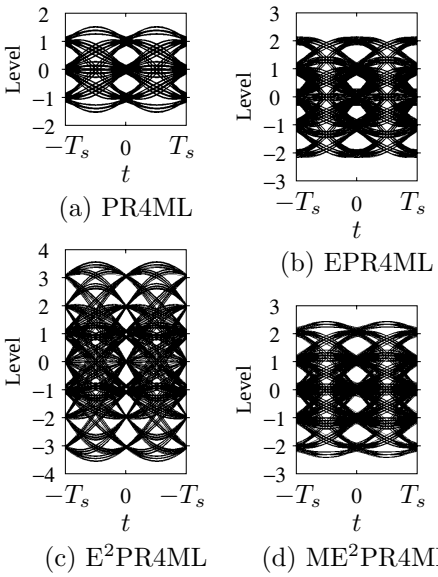

(a) PR4ML (b) EPR4ML

(c) E^{2}PR4ML (d) ME^{2}PR4ML

Fig. 3 Eye patterns of PRML systems for the 8/9 code ($\beta = 0.5$, $\eta = \eta_{\rm opt}$).

PR(1, 2, 3, 2, 1)ML have good eye openings and phase margins.

IV. NOISE POWER SPECTRA

The one-sided power spectrum of noise at the discrimination point is obtained from $N_0|E(x)|^2/2$ as follows:

$$N(x) = \frac{\{\tan^{-1}(\eta_c/K_p)\}^2}{a^2} \cdot \frac{x^2R^2(x)\cdot e^{2\pi K_p x}}{\sin^2(\pi\eta_c x)} \cdot \sum_{m=0}^{L-1}\sum_{n=0}^{L-1} u_m u_n \cos 2\pi(m-n)\eta_c x \ . \quad (10)$$

Here, a is the signal-to-noise ratio (SNR) at the reading point and is defined as the ratio of the peak value of $g(t)$ to the rms value of noise in a bandwidth equal to f_b:

$$a = \frac{A}{\sqrt{N_0 f_b}}. \quad (11)$$

The noise power spectra for the (1,7) and 8/9 codes at the discrimination point are shown in Figs. 4 and 5, respectively, where $K_p = 2.5$, $\beta = 0.5$ and $\eta = \eta_{\rm opt}$. Since the levels of the eye patters in Figs. 2 and 3 are normalized by e_0/e_1, the spectra in Figs. 4 and 5 are also normalized by multiplying $(e_0/e_1)^2$. The overall spectra and their high-frequency components for the (1,7) code are small compared with those for the 8/9 code, because the value of $\eta_{\rm opt}$ for the (1,7) code is greater than that for the 8/9 code and hence the bandwidth of the equalizer for the (1,7) code is narrow compared with that for the 8/9 code. Among PRML systems for the (1,7) code, PR(1, 2, 1)ML has the minimum spectrum. This is followed by PR(1, 2, 2, 1)ML, PR(1, 2, 3, 2, 1)ML and PR(1, 3, 3, 1)ML. On the other hand, among PRML systems for the 8/9 code, ME^{2}PR4ML has the minimum spectrum, and this is followed by EPR4ML, E^{2}PR4ML and PR4ML.

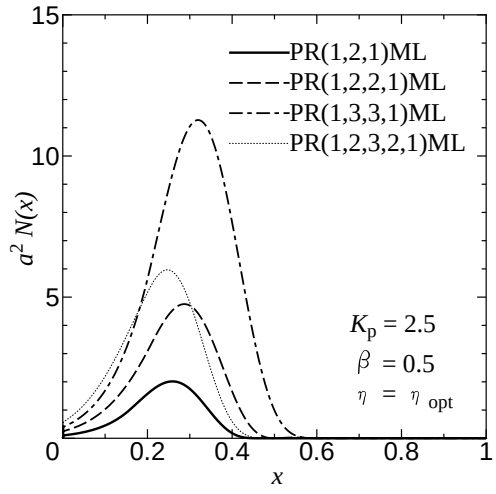

Fig. 4 Power spectra of noise at the discrimination point of PRML systems for the (1,7) code.

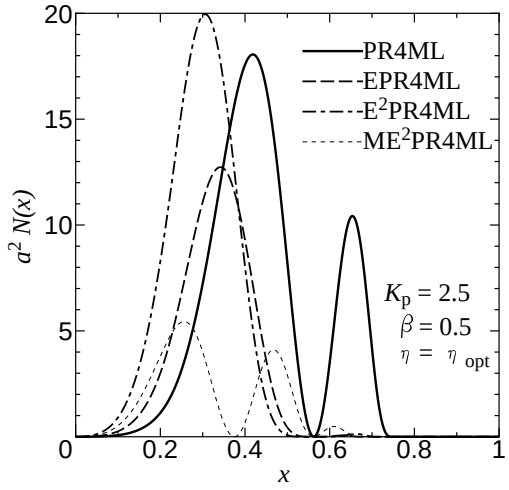

Fig. 5 Power spectra of noise at the discrimination point of PRML systems for the 8/9 code.

V. PRML SYSTEMS

The input signal sequence of the Viterbi detector is obtained by sampling $y(t)$ at $t = kT_s$ as follows:

$$d_k = y(kT_s) = \sum_i (2c_i - 1)w\big((k-i)T_s\big) \ . \quad (12)$$

Here, we describe the Viterbi detection in PR(1, 2, 2, 1)ML as an example of PRML system for the (1,7) code. As the run-length of 1's or 0's in the precoder output sequence $\{c_k\}$ for the (1,7) code is limited to from 2 to 8, the sequences 010 and 101 do not appear in $\{c_k\}$. Taking account of this constraint, we have the state assignment table at $t = kT_s$ shown in Table 3. It is evident from Eqs. (4), (5) and (12) that the input signal sequence $\{d_k\}$ of the detector for $\eta = \eta_c$ is given by

$$d_k = c_k + 2c_{k-1} + 2c_{k-2} + c_{k-3} - 3 \ . \quad (13)$$

Table 3 State assignment table of PR(1,2,2,1)ML for the (1,7) code.

State	c_{k-2}	c_{k-1}	c_k
S_0	0	0	0
S_1	0	0	1
S_2	0	1	1
S_3	1	0	0
S_4	1	1	0
S_5	1	1	1

Table 4 State transition table of PR(1,2,2,1)ML for the (1,7) code.

Previous state	c_k	Present state		d_k	
		0	1	0	1
S_0		S_0	S_1	–3	–2
S_1		—	S_2	—	0
S_2		S_4	S_5	1	2
S_3		S_0	S_1	–2	–1
S_4		S_3	—	0	—
S_5		S_4	S_5	2	3

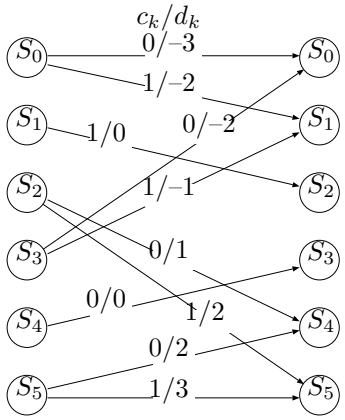

Fig. 6 Trellis diagram of PR(1,2,2,1)ML for the (1,7) code.

Using this equation and the above-mentioned constraint on the minimum run-length, we have the state transition table shown in Table 4. From Table 4, we can obtain the trellis diagram shown in Fig.6 where each branch is labeled with c_k/d_k. By defining the length of each branch on the trellis diagram by the negative log-likelihood function, the metrics for the states $S_0 \sim S_5$ at time $t = kT_s$ are obtained from Fig.6 [13]. The Maximum-likelihood sequence $\{\hat{c}_k\}$ can be determined by tracing back in the past the paths survived by the minimum value selection in the metric. Further, by means of the operation given by Eq.(8), the input sequence of the decoder $\{\hat{b}_k\}$ is obtained.

Table 5 $d^2_{\min}$, number of states (ACS's), and signal levels for PRML systems.

PRML System	$d^2_{\min}$	Number of states (ACS's)	Signal levels
PR(1, 2, 1)ML	6	4(2)	4
PR(1, 2, 2, 1)ML	10	6(4)	7
PR(1, 3, 3, 1)ML	20	6(4)	7
PR(1, 2, 3, 2, 1)ML	18	10(6)	10
PR4ML	2	2×2(2×2)	3
EPR4ML	4	8(8)	5
E^2PR4ML	6	16(16)	7
ME^2PR4ML	2	16(16)	5

A Viterbi detector for the (1,7) code can be formed from metrics [13],[14]. By using the minimum run-length constraint of the (1,7) code, the number of states can be reduced from 8 to 6, which contributes to the simplification of the detector. The minimum run-length constraint of the (1,7) code also brings the effect that the ACS (Add-Compare-Select) number is reduced from 8 to 4. Another important effect of run-length constraint is that the increase in the minimum Euclidean distance $d_{\min}$ between all possible pairs of sequences in $\{d_k\}$ brings the improvement in BER performance. For the other PRML systems, we can form Viterbi detectors using the run-length constraint of the (1,7) code in a similar way.

For the case of the 8/9 code, we cannot exploit the run-length constraint, so that we do not have the reduction in the numbers of states and ACS's and the increase in $d_{\min}$. $d^2_{\min}$, the number of states (ACS's) and signal levels are shown in Table 5. PR(1, 2, 1)ML, PR(1, 2, 2, 1)ML and PR(1, 3, 3, 1)ML for the (1,7) code can attain large $d^2_{\min}$ with the small numbers of states and ACS's compared with PRML systems for the 8/9 code.

VI. PERFORMANCE COMPARISON

The BER performance of PRML systems for the (1,7) and 8/9 codes obtained by computer simulation is shown in Fig.7 where $K_p = 2.5$, $\beta = 0.5$ and $\eta = \eta_{\text{opt}}$. In the figure, the symbols ○, △, □ and ◇ indicate the performance of PR(1, 2, 1)ML, PR(1, 2, 2, 1)ML, PR(1, 3,

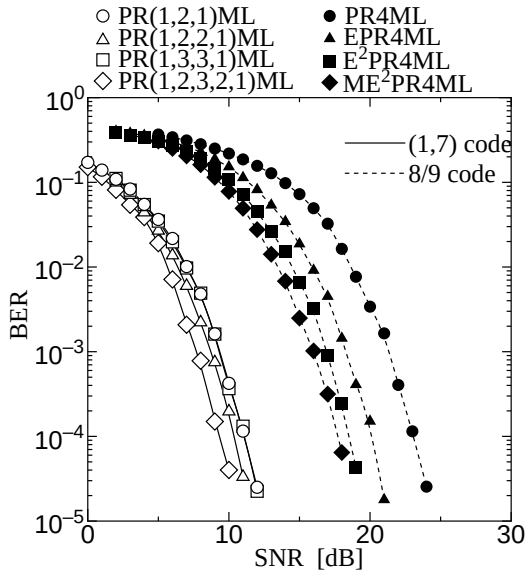

Fig. 7 BER performance ($K_p = 2.5$, $\beta = 0.5$, $\eta = \eta_{\rm opt}$).

3, 1)ML and PR(1, 2, 3, 2, 1)ML for the (1,7) code, respectively. Also, the symbols ●, ▲, ■ and ◆ indicate the performance of PR4ML, EPR4ML, E^2PR4ML and ME^2PR4ML for the 8/9 code, respectively. As can be seen in the figure, the performance for the (1,7) code are better than that for the 8/9 code. Among these PRML systems, PR(1, 2, 3, 2, 1)ML shows the best performance. This is followed by PR(1, 2, 2, 1)ML, PR(1, 3, 3, 1)ML, PR(1, 2, 1)ML, ME^2PR4ML, E^2PR4ML, EPR4ML and PR4ML. When the input noise of the detector is a white Gaussian noise, the SNR gain of Viterbi detection over the threshold detection is approximated as follows [15]:

$$\mathrm{SNR_G} \simeq 10\log_{10} d^2_{\rm min} \quad [\mathrm{dB}]\ . \tag{14}$$

Actually, the input noise sequence is the colored noise sequence characterized by the transfer function of the equalizer. Therefore, $\mathrm{SNR_G}$ can be degraded by the influence of its correlation. However, we can roughly evaluate the performance of PRML systems by using $\mathrm{SNR_G}$. $\mathrm{SNR_G}$ of each PRML system can be obtained by substituting $d^2_{\rm min}$, given by Table 5, into Eq.(14). PR(1, 2, 3, 2, 1)ML and PR(1, 2, 2, 1)ML for the (1,7) code have small noise spectra and large $\mathrm{SNR_G}$'s, which results in excellent performance. PR(1, 3, 3, 1)ML shows comparative good performance despite its large

Table 6 SNR improvement of each PRML system over PR4ML (K_p=2.5, β=0.5,η=$\eta_{\rm opt}$,BER=10^{-4}).

(1,7) code		8/9 code	
PRML system	$\mathrm{SNR_I}$ [dB]	PRML system	$\mathrm{SNR_I}$ [dB]
PR(1,2,1)ML	11.9	EPR4ML	2.9
PR(1,2,2,1)ML	12.5	E^2PR4ML	4.6
PR(1,3,3,1)ML	11.9	ME^2PR4ML	5.5
PR(1,2,3,2,1)ML	13.8		

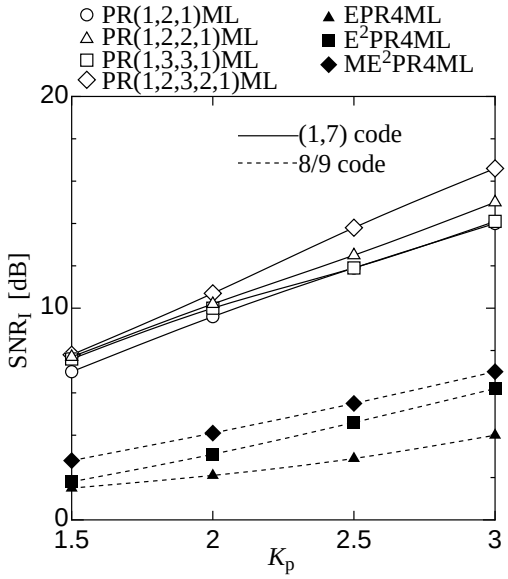

Fig. 8 SNR improvement of each PRML system over PR4ML ($\beta = 0.5$, $\eta = \eta_{\rm opt}$, $\mathrm{BER} = 10^{-4}$).

noise spectrum, because it has the best $\mathrm{SNR_G}$ among PRML systems studied here. PR(1, 2, 1)ML having the minimum noise spectrum also shows good performance. Table 6 shows the SNR improvement $\mathrm{SNR_I}$ of each PRML system over PR4ML obtained by Fig.7 where $K_p = 2.5$, $\beta = 0.5$, $\eta = \eta_{\rm opt}$ and $\mathrm{BER} = 10^{-4}$.

Fig.8 shows the relationship between the normalized linear density K_p and the SNR improvement of each PRML system over PR4ML where $\beta = 0.5$, $\eta = \eta_{\rm opt}$ and $\mathrm{BER} = 10^{-4}$. PR(1, 2, 3, 2, 1)ML exhibits the maximum SNR improvement over all the density of $1.5 \le K_p \le 3$. The SNR improvement of each PRML system increases with the increase in the linear density.

VII. CONCLUSION

PRML systems for the combination of an MR head and a double layer perpendicular medium have been

investigated. The BER performance of PRML systems with the positive coefficients for the (1,7) code and the negative coefficients for the 8/9 code has been evaluated. The PRML system for the (1,7) code has a large minimum Euclidean distance and a small noise spectrum compared with those for the 8/9 code, which results in a significant performance improvement. Among PRML systems discussed in this study, PR(1, 2, 3, 2, 1)ML for the (1,7) code exhibits the best performance and improves the SNR by about 13.8 dB over that of PR4ML for the 8/9 code at a BER of 10^{-4} and a normalized linear density of 2.5. This can be achieved at the expense of some increase in complexity of the Viterbi detector. PR(1, 2, 2, 1)ML, PR(1, 3, 3, 1)ML and PR(1, 2, 1)ML also provide excellent performance. PR(1, 2, 1)ML gains about 11.9 dB in SNR with the comparable complexity to PR4ML.

ACKNOWLEDGEMENT

The authors wish to thank Prof. S. Tazaki of Ehime University for his helpful discussion. This work was supported in part by the Grant-in-Aid of the Storage Research Consortium, Japan.

REFERENCES

[1] R.W.Wood and D.A.Petersen, "Viterbi Detection of Class IV Partial Response on a Magnetic Recording Channel," IEEE Trans. Commun., vol. 34, pp. 454–461, May 1986.

[2] H.K.Thapar and A.M.Patel, "A Class of Partial Response Systems for Increasing Storage Density in Magnetic Recording," IEEE Trans. Magn., vol. MAG-23, pp. 3666–3668, Sept. 1987.

[3] T.D.Howell, D.P.McCown, T.A.Diola, Y.Tang, K. R.Hense and R.L.Gee, "Error Rate Performance of Experimental Gigabit per Square Inch Recording Components," IEEE Trans. Magn., vol. 26, pp. 2298–2302, Sept. 1990.

[4] Y. Sonobe, Y. Ikeda, H. Uchida and T. Toyooka, "High-density Recording Characterization Using a Merged MR Head and a Dual-layer Perpendicular Disk," IEEE Trans. Magn., vol. 31, pp. 2681 –2683, Nov. 1995.

[5] S.Ohki, T.Okumura, H.Matsutera and K.Tagami, "Read / Write Characteristics of Perpendicular Magnetic Media with ID/MR Composite Head," J. Mag. Soc. Japan, vol. 19, Suppl. no. S2, pp. 122–125, Oct. 1995.

[6] H. Muraoka, H. Yamada and Y. Nakamura, "MR Head Reading Characteristics in Perpendicular Magnetic Recording," IEEE Trans. Magn., vol. 32, pp. 3482–3484, Sept. 1996.

[7] M. Futamoto, Y. Honda, Y. Hirayama, K. Itoh, H. Ide and Y. Maruyama, "High Density Magnetic Recording on Highly Oriented CoCr-Alloy Perpendicular Rigid Disk Media," IEEE Trans. Magn., vol. 32, pp. 3789–3794, Sept. 1996.

[8] K. Ho, L. Mei, K. Schouterden, N. Li and B. M. Lairson, "Recording Performance of High Remanence Perpendicular CoCrTa/Pt Multilayers," Digests of INTERMAG'97, GB-03, 1997.

[9] H.Ide, "A Modified PRML Channel for Perpendicular Magnetic Recording," IEEE Trans. Magn., vol. 32, pp. 3965–3967, Sept. 1996.

[10] D. J. Seagle, M. A. Meininger, T. J. Beaulieu and C. J. Spector, "Recording Performance of an Inductive-write,Wide-shielded MR Readback Head with a Dual Layer Perpendicular Disk," IEEE Trans. Magn., vol.26, pp.2160–2162, Sept. 1990.

[11] H.Osawa, M.Okada, K.Wakamiya and Y.Okamoto, "Performance Improvement of PRML System for (1,7) RLL Code," IEICE Trans. Electron., vol. E79-C, pp. 1455–1461, Oct. 1996.

[12] H.Osawa, S.Yamashita and S.Tazaki, "Improvement on Error Rate Performance for FM Recording Code," IEEE Trans. Magn., vol. MAG-27, pp. 4464–4469, Nov. 1991.

[13] H. Kobayashi, "Application of Probabilistic Decoding to Digital Magnetic Recording Systems," IBM J. Res. & Dev., vol. 15, pp. 64–74, 1971.

[14] M.J.Ferguson, "Optimal Reception for Binary Partial Response Channels," BSTJ, vol. 51, pp. 493 –505, Feb. 1972.

[15] G.D.Forney, Jr., "Mamimum-Likelihood Sequence Estimation of Digital Sequences in the Presence of Intersymbol Interference," IEEE Trans. Inf. Theory, vol. IT-18, pp. 364–378, May 1972.